Fixed Winding Number and the Quasiperiodic Route to Chaos in a Convective Fluid

J. Stavans, F. Heslot, and A. Libchaber
The James Franck Institute and The Enrico Fermi Institute, The University of Chicago, Chicago, Illinois 60637
(Received 19 April 1985)

We present an experimental observation of the transition to chaos for quasiperiodic routes of fixed winding number. The hydrodynamical system studied is a Rayleigh-Bénard experiment in mercury, in a time-dependent state with one limit cycle. A second oscillator is imposed by an ac current. We have measured the fractal dimension of the locked regions at the critical curve as well as the scaling properties associated with two different irrational winding numbers, to which the system was tuned. Our results agree with quantitative theoretical predictions based on the circle map.

PACS numbers: 47.20.+m, 47.25.−c

In low-order dynamical systems, a quantitative set of predictions and observations exist for the case of successive period-doubling bifurcations.[1,2] Theoretical predictions exist also for the transition from quasiperiodicity to chaos, using renormalization-group methods.[3–6]

In this paper we report quantitative results on a fluid flow experiment addressing the question of quasiperiodicity. We study a flow with two sharp frequencies, in a Rayleigh-Bénard experiment. Usually, when the two frequencies are generated by the flow, an increase in a control parameter results in mode locking. That is, the ratio of the two basic frequencies retains a given rational value over some finite range of the control parameter. To study a quasiperiodic flow with incommensurate frequencies, a practical approach is to start from a state of the fluid with one oscillator present, and to force a second oscillator by modulating a control parameter. In this way one can achieve any desired ratio of frequencies between the two oscillators. One can study the transition from quasiperiodicity to chaos by increasing the nonlinearities in the flow. In the present work we keep the Rayleigh number fixed, and we increase the nonlinearities by increasing the amplitude of the forced oscillator. The existing theoretical predictions pertain to a route to chaos in which the frequency ratio of the oscillators, the winding number, is kept constant and as close as possible to an irrational value. The irrational value usually chosen is the golden mean $\sigma_G = (\sqrt{5}-1)/2$. It has a periodic representation as a continuous fraction containing only ones $\langle 1, 1, 1, 1, \ldots \rangle$ and has, therefore, the slowest possible convergence in a rational approximation. Preliminary experimental results on this route have already been obtained.[7] In our experiment we followed two routes, setting the winding number either to the golden mean, or to the "silver mean" $\sigma_S = \sqrt{2}-1$ defined by $\langle 2, 2, 2, 2, \ldots \rangle$ in continued-fraction representation.

Small-aspect-ratio Rayleigh-Bénard experiment in mercury.—We will not describe the experimental setup already published elsewhere.[2] We used a small-aspect-ratio cell ($0.7 \times 0.7 \times 1.4$ cm^3) filled with mercury. For low-Prandtl-number fluids like mercury, the first bifurcation above the onset of convection in a Rayleigh-Bénard experiment is a Hopf bifurcation which leads to a time-dependent state called the oscillatory instability.[8] This instability is our first oscillator and is related to the appearance of ac vertical vorticity in the fluid.[9]

Our second oscillator is generated in the fluid by an electromagnetic process. We apply a small dc magnetic field, horizontal and parallel to the axis of the convective cells in the fluid ($H = 200$ G). We apply a vertical ac sheet of current through the fluid, on the plane separating the two convection rolls which are in the cell (I of the order of 20 mA). The plane of the current is parallel to the magnetic field. The Lorenz force induces an ac vertical vorticity in the fluid's velocity field. This is our second oscillator, whose frequency and amplitude are controlled externally. We use a pulse excitation, the pulse width being about $\frac{1}{10}$ of the period. A pulse excitation was used instead of a sinusoidal one to allow some degrees of freedom to the fluid velocity field. Changing the amplitude and frequency of the ac current we can scan a very large range of winding numbers and amplitudes. We note that in this experiment with two competing oscillators, one is fixed externally and the other, the oscillatory instability, is shifted in frequency and amplitude by the former. This is different from a situation where two oscillators can freely interact and both frequencies and amplitudes can shift. The fluid motion is measured locally with a thermal probe located in the bottom plate of the cell. In a small-aspect-ratio cell, the location of the detector is irrelevant. The winding number and the oscillators' amplitudes are measured using a fast-Fourier-transform analysis of the data. The quality of such an experiment depends on the stability achieved. The internal oscillator frequency is close to 0.230 Hz and its stability is 10^{-5}. The generator used for the imposed frequency is an HP 3325A which has a stability well beyond our needs.

Quasiperiodicity and phase lock-in.—By sweeping the external frequency and amplitude one can map out a number of phase-locked states, the so-called Arnold

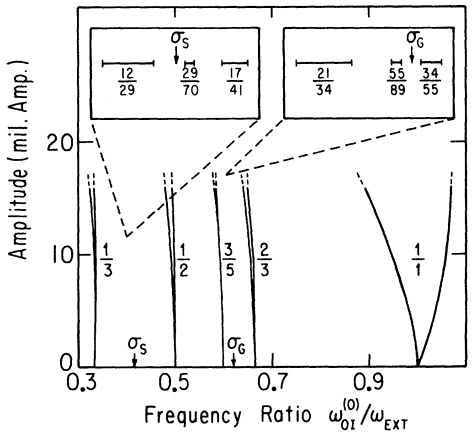

FIG. 1. Locked-mode regions (Arnold tongues) in a diagram of external pulse amplitude vs the ratio of the frequency of the oscillatory instability (at zero forcing) $\omega_{01}^{(0)}$ to the frequency of the external pulses ω_{ext}. Only tongues of appreciable width are shown. The frequency ratio is given for these tongues. Insets: Locked states near σ_G and σ_S (Ref. 12) on the critical line. The origin of each inset shows the position of the critical line at the particular irrational frequency ratio and the precise frequency limits of each locked state are given in Table I.

tongues.[10] The results are depicted in Fig. 1. The horizontal scale is the ratio between the "bare" oscillatory instability frequency $\omega_{01}^{(0)}$ (zero external excitation) and the external frequency. On the vertical axis we have plotted lock-in regions with large widths, corresponding to small denominators in the frequency ratio. Locked states with denominators larger than 200 have been observed and are stable. As theoretically predicted, the width of the tongues grows with the amplitude of the excitation. Eventually the tongues overlap, the critical amplitude for overlapping depending on the frequency ratio. This defines a critical curve on our diagram: On this curve (henceforth called the "critical line") the locked bands, which are ordered through the Farey construction,[11] form a Cantor-type set with fractal dimension D.

We measured D near σ_G and σ_S as follows[12,13]: Denote by S the length of the interval between two locked-band parents around the irrational winding number being considered. This interval includes inside it the locked daughter band corresponding to the Farey composition of the parent states. Denote by S_i, $i=1,2$, the length of the intervals between the daughter band and each parent, respectively. Then D is given by

$$(S_1/S)^D+(S_2/S)^D\approx 1.$$

In the insets in Fig. 1 we show the bands used to compute D for each of the two irrationals; Table I indicates the bands' frequency limits. The critical line is not a constant-amplitude line in the diagram, even for measurements made at the same Rayleigh number. The critical amplitude depends on the irrational frequency ratio chosen. This dependence is indicated in the figure by the different origins of the insets. The amplitudes in the figure correspond to a Rayleigh number $R=4.09R_c$.

Our results for D are shown in Table II. In the case of σ_G, the result is an average over two of the possible combinations obtained from the four locked bands. Up to experimental error (3%), the result of the measurements at both σ_G and σ_S is the same, showing that D is indeed a global property along the critical line. Moreover, our results agree well (2%) with the theoretical result[10,14] $D=0.868$.

Scaling properties of the routes with fixed winding number.—To follow a route of fixed frequency ratio the experimental procedure is as follows: We increase the excitation amplitude by a small amount and then adjust the external frequency so that the ratio between the two frequencies remains constant up to 0.03%. This is done by means of a fast-Fourier-transform analysis of the temperature signal. The Rayleigh number is kept fixed during the experiment. It is evidently nonphysical to stay at an irrational value and the best we can do is to approximate it to within 2×10^{-4}.

From the study close to the golden mean, $\sigma_G=(\sqrt{5}-1)/2$, we show in Fig. 2 three spectra

TABLE I. Frequency limits of locked states near σ_G and σ_S (Ref. 12) at the nearest approximation to the critical line. The data were taken at $A=17.4$ mA for σ_G and $R=4.09R_c$ while for σ_S, $A=19.4$ mA and $R=3.94R_c$. The uncertainty in the data is 5% of the locked bands' widths.

Locked state	σ_{low} (MHz)	σ_{high} (MHz)
	$\sigma_G=\langle 1,1,1,1,\ldots\rangle$	
13/21	392.350	392.663
21/34	393.230	393.345
34/55	393.050	393.095
55/89	393.133	393.155
	$\sigma_S=\langle 2,2,2,2,\ldots\rangle$	
12/29	574.175	574.575
17/41	573.450	573.650
29/70	573.865	573.925

TABLE II. Experimental data for the fractal dimension D of the critical line and the scaling number δ near σ_G and σ_S (Ref. 12) at the corresponding critical amplitudes.

	$\sigma_G=\langle 1,1,1,1,\ldots\rangle$	$\sigma_S=\langle 2,2,2,2,\ldots\rangle$
D	$0.86\pm3\%$	$0.85\pm3\%$
δ	$2.8\pm10\%$	$7.0\pm10\%$

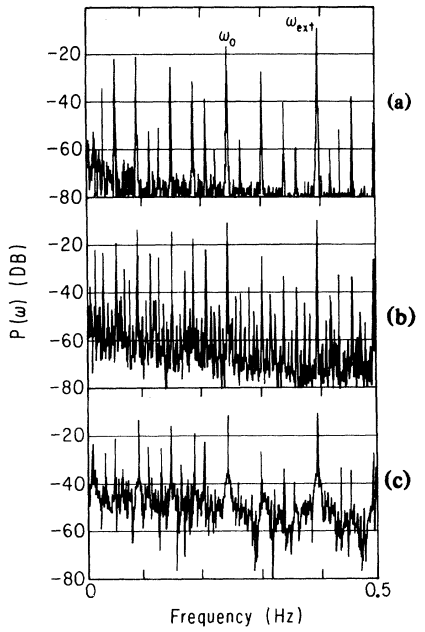

FIG. 2. Spectra, $\log P(\omega)$ vs ω, for quasiperiodic states at $R = 4.09R_c$ having frequency ratio σ_G (with 2×10^{-4} accuracy) between the renormalized oscillatory instability frequency ω_0 and the external pulse frequency ω_{ext}, at different pulse amplitudes: (a) $A = 16.9$ mA (below the critical line), (b) $A = 17.4$ mA (nearest approximation to the critical line), (c) $A = 21.5$ mA (above the critical line).

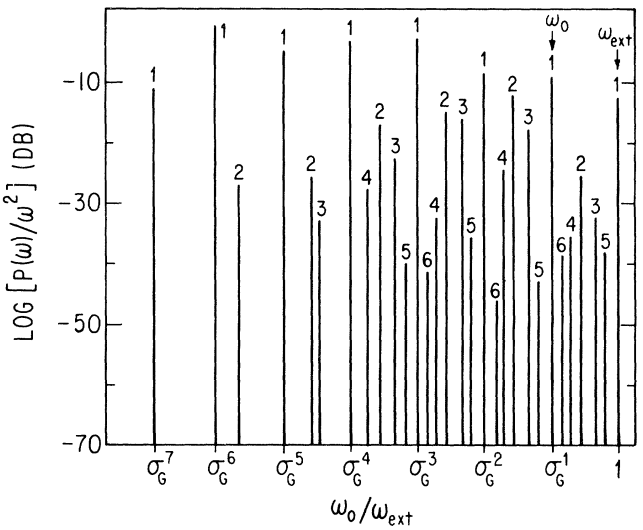

FIG. 3. Scaled spectrum for frequency ratio $\omega_0/\omega_{ext} = \sigma_G \pm 2\times10^{-4}$ and pulse amplitude $A = 17.4$ mA (nearest approximation to critical line), where ω_0 is the renormalized oscillatory instability frequency and ω_{ext} the external pulse frequency. We plot $\log[P(\omega)/\omega^2]$ vs $\log\omega$. The spectrum corresponds to that of Fig. 2(b); not all peaks are shown for the sake of clarity. Each peak is labeled by an integer showing to which generation it belongs.

below, at, and above the critical point. The main observations are as follows: Below the critical line, Fig. 2(a), a small number of peaks appear, all linear combinations of our two basic frequencies ω_{ext} and ω_0. At the critical line, Fig. 2(b), a very large increase of combination frequencies is observed in the spectrum. Slightly above the critical line, high-order combination frequencies are weaker and noise is present with the average noise level increased by almost 20 dB. This route to chaos shows some qualitative behavior similar to period doubling. Up to the critical point the low-frequency population increases with the control parameter. Above this critical value noise slowly replaces the higher combination frequencies. Close to the golden mean the Fourier spectrum can be redrawn to show self-similarity. We have plotted, in Fig. 3, $\log[P(\omega)/\omega^2]$ vs $\log(\omega)$, at the critical point corresponding to Fig. 2(b). For the sake of clarity not all the peaks experimentally observed are shown. The peaks labeled 1 can be obtained from the internal frequency ω_0 by the prescription $\omega = \omega_0\sigma_G^n$.

In fact, all the peaks in generation 1 are obtained by the formula $\omega = |m\sigma_G - n|$ (with the external frequency normalized to 1), where m,n ($m > n$) are successive numbers of the main Fibonacci sequence $(1, 1, 2, 3, 5, 8, \ldots)$. The same prescription accounts for all the peaks of the spectrum, each integer-labeled generation obtained from a different seed in a Fibonacci sequence. For example, generation 2 is obtained using the seed (2,2), generation 3 using (1,3), generation 4 using (3,3) and so on. In our nearest approximation to the critical line, Fig. 2(b), more generations appear in the spectrum and generation 10 can be identified, although not at the lowest frequencies.

The spectrum in Fig. 3 is divided into bands, each of which is flanked by two adjacent first-generation peaks. The amplitude of the peaks of generation 1 is nearly constant, although the amplitude of the last peak is smaller. For generation 2 the decrease in amplitude starts earlier. So at least for the first generation, in this scale representation at the critical point, the theoretically predicted constant amplitude is observed.

As in the case of the period-doubling route to chaos, renormalization-group and numerical studies of circle maps have shown the existence of two numbers,[3-6] which reflect the scaling properties of particular irrational routes with periodic continued-fraction representations. These numbers, α and δ, have values which depend on the irrational number chosen. α appears in the fixed-point equation while δ is the scale factor by which tongue widths change. More precisely, if n denotes the nth truncation of the continued fraction representation of an irrational, and Ω_n represents the width of the locked state at the critical amplitude,

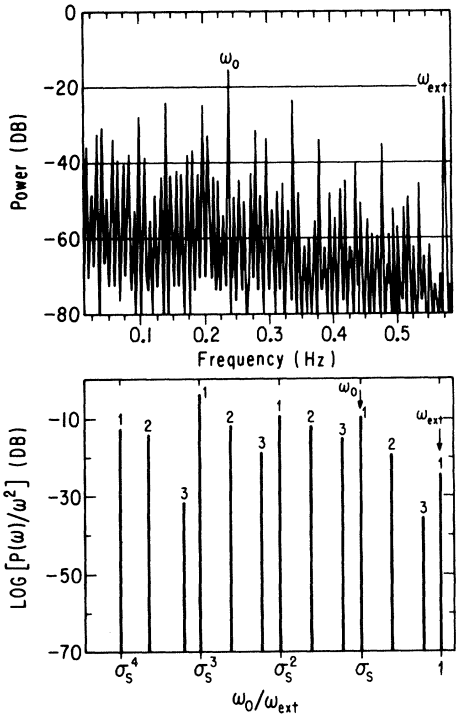

FIG. 4. Spectrum and its scaled version (up to generation 3) for a quasiperiodic state with frequency ratio $\sigma_S \pm 2\times 10^{-4}$ and external pulse amplitude $A = 25.2$ mA. This corresponds to our nearest approximation to the critical line at this winding number. For this spectrum $R = 3.98R_c$.

then

$$\delta = \lim_{n\to\infty} \frac{\Omega_{n-1} - \Omega_n}{\Omega_n - \Omega_{n+1}}.$$

We have measured δ for both σ_G and σ_S[12] and our results are shown in Table II. Our values agree well with the theoretical ones[3–6]: $\delta = 2.833\ldots$ for σ_G while $\delta = 6.799$ for σ_S.

Figure 4 shows the Fourier spectrum and the scaled spectrum for σ_S at the critical point. It shows the same self-similarity observed for σ_G. Unfortunately, α cannot be calculated simply by composing the relative heights of lines in the spectrum as in the case of period doubling,[1] and we have not yet been able to extract it from our data.

Finally, our experiment demonstrates that the critical value of the forced-oscillator amplitude is larger for the golden mean than for the silver mean, as shown in the insets of Fig. 1. In the Arnold diagram the critical region is thus a curve, whose maximum may occur at the golden mean.

This work is the first quantitative study of the commensurate-incommensurate transition for quasiperiodicity. Its experimental precision allows a detailed study of this rich dynamical system. We are now concentrating on the supercritical region which allows the measurements of α,[15] of the scaling of the Lyapounov exponent, and a careful study of the fine structure of phase locking.[16,17] We expect a new behavior to appear far from the critical line.

Extremely useful discussions with J. Gollub, M. Jensen, L. Kadanoff, I. Procaccia, B. Shraiman, and S. Thomae are acknowledged. This work was supported by the National Science Foundation under Grant No. DMR-83 16204 and partly by the Materials Research Laboratory at the University of Chicago under National Science Foundation Grant No. DMR 82-16892.

[1]M. J. Feigenbaum, Phys. Lett. **74A**, 375 (1979); M. J. Feigenbaum, J. Stat. Phys. **19**, 25 (1978), and **21**, 669 (1979); M. J. Feigenbaum, in *Nonlinear Phenomena in Chemical Dynamics,* edited by C. Vidal and A. Pacault (Springer, Berlin, 1981), pp. 95–102.

[2]A. Libchaber, C. Laroche, and S. Fauve, Physica (Amsterdam) **7D**, 73 (1983), and J. Phys. (Paris), Lett. **43**, L211 (1982).

[3]S. J. Shenker, Physica (Amsterdam) **5D**, 405 (1982).

[4]M. J. Feigenbaum, L. P. Kadanoff, and S. J. Shenker, Physica (Amsterdam) **5D**, 370 (1982).

[5]D. Rand, S. Ostlund, J. Sethna, and E. Siggia, Phys. Rev. Lett. **49**, 132 (1982), and Physica (Amsterdam) **6D**, 303 (1984).

[6]B. Shraiman, Phys. Rev. A **29**, 3464 (1984).

[7]A. P. Fein, M. S. Heutmaker, and J. P. Gollub, Phys. Scr. **T9**, 79 (1985).

[8]F. H. Busse, Rep. Prog. Phys. **41**, 1929 (1978).

[9]E. D. Siggia and A. Zippelius, Phys. Rev. Lett. **47**, 835 (1981).

[10]M. H. Jensen, P. Bak, and T. Bohr, Phys. Rev. Lett. **50**, 1637 (1983), and Phys. Rev. A **30**, 1960 (1984).

[11]T. Allen, Physica (Amsterdam) **6D**, 305 (1983).

[12]The critical amplitude for σ_S was found for $R = 4.09R_c$ as for σ_G, whereas the data for computing scaling properties and the fractal dimension of the critical line near σ_S were taken at $R = 3.94R_c$.

[13]H. G. E. Hentschel and I. Procaccia, Physica (Amsterdam) **8D**, 435 (1983).

[14]P. Cvitanovic, M. H. Jensen, L. P. Kadanoff, and I. Procaccia, Phys. Rev. Lett. **55**, 343 (1985).

[15]T. Bohr, to be published.

[16]L. Glass and R. Perez, Phys. Rev. Lett. **48**, 1772 (1982).

[17]D. G. Aronson, M. A. Chory, G. R. Hall, and R. P. McGehee, Commun. Math. Phys. **83**, 355 (1982).